Human Cell (2021) 34:122–131
https://doi.org/10.1007/s13577-020-00412-z

RESEARCH ARTICLE

# Circ-XPR1 promotes osteosarcoma proliferation through regulating the miR-214-5p/DDX5 axis

**Xiaohuan Mao[1] · Shuren Guo[2,3] · Lan Gao[1] · Gang Li[1]**

Received: 9 June 2020 / Accepted: 7 August 2020 / Published online: 12 September 2020


## Abstract

Circular RNAs (circRNAs) are a new class of RNAs that play an important role in the development of various tumors. However, the expression profile and biological function of circRNAs in osteosarcoma (OS) progression remain unclear. OS-related circRNA expression profiles from the GEO database (GSE96964) were downloaded to identify differentially expressed circRNAs between OS and normal tissues. We identified one upregulated circRNA (Circ-XPR1), and RT-PCR was performed to further confirm the expression abundance in OS tissue. Circ-XPR1 was closely related to overall survival and disease-free survival of OS patients. Knockdown of Circ-XPR1 significantly reduced the proliferation of OS cells. Gain- and loss-of-function studies showed that Circ-XPR1 promoted OS cell proliferation by sponging miR-214-5p to regulate *DDX5* expression. Our findings suggested that Circ-XPR1 regulates OS cell proliferation by sponging miR-214-5p to regulate *DDX5* expression. Therefore, the Circ-XPR1/miR-214-5p/*DDX5* axis may serve as a potential therapeutically relevant target for OS.

**Keywords** Circ-XPR1 · miR-214-5p · DDX-5 · Osteosarcoma

## Introduction

Osteosarcoma (OS) is the most common malignant tumor of bone and mainly affects children and adolescents [1]. The annual incidence of OS is 4–5 cases per 1,000,000 individuals worldwide [2]. Despite development of OS treatment approaches, such as chemotherapy and curative resection, OS overall survival is poor [3]. The molecular mechanism underlying OS development remains unclear [4]. Therefore, in-depth exploration of the mechanism underlying OS development is important to develop effective preventions and therapies.

Circular RNAs (circRNAs) are recently identified molecules classified into a type of noncoding RNAs. CircRNAs show diverse biological functions, including cellular proliferation, invasion and metastasis [5]. CircRNAs function by serving as miRNA sponges and subsequently regulating target gene expression [6]. Several studies have explored the role of circRNAs in OS. Fang et al. [7] demonstrated that circ_0000337 is significantly upregulated in OS cell lines and promotes OS progression via the miR-4458/*BACH1* pathway. Another study conducted by Zhang et al. [8] revealed that has_circ_0002052 stimulates the progression of OS through sponging miR-382. To date, however, the potential mechanisms of circRNAs in OS progression have rarely been studied.

MicroRNAs (miRNAs) are noncoding RNAs that mainly function as inhibitors of target genes [9]. MiRNAs affect the biological behaviors of multiple cancers, including OS. Liu et al. [10] revealed that miR-874-3p inhibits OS cell line migration through targeting *RGS4*. Further studies on miRNA and OS progression are required. In recent years, a number of tumor-related databases have been established, including Gene Expression Omnibus (GEO) and TCGA.

**Electronic supplementary material** The online version of this article (https://doi.org/10.1007/s13577-020-00412-z) contains supplementary material, which is available to authorized users.

✉ Gang Li
lim5345@163.com

[1] Department of Clinical Laboratory, Henan Provincial People's Hospital, People's Hospital of Zhengzhou University, Zhengzhou 450003, Henan, People's Republic of China

[2] Department of Clinical Laboratory, The First Affiliated Hospital of Zhengzhou University, East Jianshe Road #1, Zhengzhou 450002, Henan, People's Republic of China

[3] Key Clinical Laboratory of Henan Province, Zhengzhou, Henan, People's Republic of China

In this study, differential gene expression analyses involving OS samples were performed using GEO datasets. We validated one circRNA, named Circ-XPR1, generated from exons 8 and 9 of the XPR1 gene. Furthermore, we demonstrated that Circ-XPR1 facilitates OS cell proliferation by sponging miR-214-5p to regulate *DDX5* expression.

## Methods

### Analysis of GEO expression dataset

The following three datasets from the GEO expression dataset were obtained from the GEO database (https://www.ncbi.nlm.nih.gov/geo/, Access date: 15 April 2020): GSE96964, GSE65071, and GSE12865. The GSE96964 dataset contains circRNA expression profiles, including one human osteoblast hFOB1.19 cell line and seven human osteosarcoma cell lines (U2OS, U2OS/MTX300, HOS, MG63, 143B, ZOS, and ZOSM). The GSE96964 platform consisted of the Agilent-069978 Arraystar Human CircRNA Microarray V1. The GSE65071 dataset contains miRNA expression profiles, containing 20 OS samples and 15 healthy controls. The GSE65071 platform consisted of the Exiqon Human V3 MicroRNA PCR Panel I + II. The GSE12865 dataset contains 12 OS samples and 2 normal human osteoblasts (HOB) samples, and the GSE12865 platform consisted of the Affymetrix Human Gene 1.0 ST Array platform.

Background correction and quantile normalization were performed for the GSE96964, GSE65071, and GSE12865 datasets using the Affy package ( https://www.bioconductor.org/) [11] and robust multiarray average (RMA) [12].

Identification of differentially expressed circRNAs, miRNAs, and mRNAs among these datasets was performed using the Limma algorithm in R [13]. For the differentially expressed analysis, the thresholds were $p$ value $< 0.05$ and logFC $> 1$ (upregulated) or logFC $< -1$ (downregulated).

To identify the targeting miRNAs of Circ-XPR1, we intersected differentially expressed miRNAs from the GSE65071 dataset, Targetscan database (https://www.targetscan.org), and miRanda database (https://www.microrna.org). Using the same method, we analyzed the miR-214-5p target gene using the intersection of GSE12865, Targetscan, miRbase, and RNAhybrid to obtain a final list of genes.

### Human tissues

In total, 20 primary OS tissues were acquired from OS patients at Henan Provincial People's Hospital between May 2011 and May 2013. All samples were confirmed by pathological diagnosis after surgery. Normal bone specimens were obtained from tissues adjacent to osteosarcoma tissues. Informed consent was obtained from all patients, and the study procedure was approved by the Ethics Committee of Henan Provincial People's Hospital. For survival analyses, the overall survival of patients was divided into low and high expression groups according to the median expression of the gene of interest, and it was presented using a Kaplan–Meier plot.

### Cell culture

Two OS cell lines (MG-63 and U2OS) were obtained from ATCC Company (Manassas, VA, USA) and maintained in a humidified incubator at 37˚C/5% $CO_2$. MG-63 and U2OS cells were cultured in Dulbecco's Modified Eagle Medium (DMEM, HyClone, Thermo-Fisher Scientific, Ottawa, ON) containing 10% fetal bovine serum, 100 U/ml penicillin G, and 100 U/ml streptomycin.

### RNA isolation of nuclear and cytoplasmic fractions

Nuclear and cytoplasmic fractions of MG-63 cells were extracted using the Nuclear and Cytoplasmic RNA Purification Kit (Cat. 21,000, Norgen, USA) according to the manufacturer's instructions. RNA extraction from nuclear and cytoplasmic fractions was performed using TRIzol reagent (Invitrogen).

### Assessment of half-life of cells

Transcription was stopped by treatment with actinomycin D (10 μg/ml), and RNA was extracted at various time points (0, 4, 8, 12 and 24 h) following actinomycin D treatment. Relative expression level of target genes was detected by qRT-PCR.

### RNA fluorescent in situ hybridization (FISH)

The Circ-XPR1 (5′-TCCCAGTGACAGTCGAATAG-3′) probe labeled with FAM was designed and synthesized by RiboBio Company (Guangzhou, China). Nuclei were stained with DAPI. The FISH experiment was performed using the BersinBio circRNA FISH Kit. Images were acquired with a confocal fluorescence microscope (Olympus Imaging, Tokyo, Japan).

### Plasmid construction

The Circ-XPR1 overexpression plasmid was designed and purchased from GenePharma (Shanghai, China) and inserted into a pcDNA3.0 vector. Empty vector (pcDNA) was used as the control. Circ-XPR1 siRNA was purchased from GenePharma (Shanghai, China). The sequences of Circ-XPR1 siRNA1 and 2 were as follows: siRNA1, 5′-AACTGCTGC TGTATTTAAACT-3′; and siRNA2, 5′-GCTGCTTAAACT

GCTGCTGTA-3′. The sequences of miR-214-5p mimic and negative control miRNA (miR-NC) were as follows: miR-214-5p mimic, 5′-ACTCCACUAGCAAACTUGAA-3′; and negative control sequence, 5′-TCAUGACGAAUGCTA GGCC-3′. siRNAs were transfected into cells using Lipofectamine 2000 Transfection Reagent (Life Technologies).

### RNase R assay and Real-time PCR

Harvested tissues or cells were placed in TRIzol® Reagent (Invitrogen). RNA samples were divided into two portions as follows: one portion was used for circRNA expression detection; and the other portion was used for GAPDH and miRNA expression measurement. Reverse transcription was performed using SuperScript III Reverse Transcriptase (Invitrogen). To purify circRNAs, 2 μg of RNA was digested with 3 U/mg Rnase R (Geneseed, Guangzhou, China) for 20 min at 37 °C. Real-time PCR analysis was performed with a PrimeScriptTM RT-PCR Kit (TaKaRa Bio Inc., Japan) on an ABI Prism 7000 sequence detection system in duplicate on two different plates. U6 or GAPDH was used as the endogenous control. The following primer sequences were used: *Circ-XPR1*: forward 5′-TGAAGAAATCGG TGCTGTGG-3′, reverse 5′- TGGTATCTCGGTTGATGT AGGT-3′; *XPR1*: forward 5′-GGCTGCGTCCTCCGACTC -3′, reverse 5′-GGGGAGAGATCACGATGTTGT-3′; *miR-214-5p*: forward 5′-ACACTCCAGCTGGGGACAAT-3′, reverse 5′-CTCAACTGGTGTCGTGGAGTCG-3′; *miR-665*: forward 5′-GGAAGAGAACTTTGCCGTTGAA-3′, reverse 5′-GTGACGAGCCATTTCCTCCTT 3′. *U6*: forward 5′-CTCGCTTCGGCAGCACA-3′; reverse 5′-AACGCTTCA CGAATTTGCGT-3′; and *GAPDH*: forward 5′-ACAACT TTGGTATCGTGGAAGG-3′; reverse 5′-GCCATCACG CCACAGTTTC-3’.

### Western blot assay

Total protein was extracted with RIPA lysis buffer (Beyotime, Shanghai, China) containing phenylmethanesulfonyl fluoride (PMSF) to measure DDX5 protein expression. Protein concentration was evaluated by a BCA Protein Assay Kit (Beyotime) following the manufacturer's protocol. Each protein sample (25 μg) was separated on a 12% SDS-PAGE gels, transferred onto a PVDF membrane (BioRad, USA), incubated with 5% no-fat milk, incubated with primary antibodies (*DDX5*, 1:1000, Abcam; and *GAPDH*, Abcam, 1:1000) overnight at 4˚C, and blocked with secondary antibodies at room temperature for 2 h. Finally, ECL detection system reagents (Millipore, MA, USA) were used to visualize the protein blots. ImageJ (National Institutes of Health, Bethesda, MD) was used to analyze the gray intensity of the bands.

### Colony formation assay

For the colony formation assay, transfected cells (1000 cells/well) were seeded into 6-well plates. After 1 week of cultivation, cells were fixed with 75% alcohol for 1 h and then stained with 0.1% crystal violet staining solution (Solarbio, Beijing, China). Colonies were quantified using ImageJ software (https://rsb.info.nih.gov/ij/).

### Cell Counting Kit-8 assay

Transfected cells were divided into the following three groups: NC group (cells transfected with scramble siRNA), siRNA-1 group (cells transfected with siRNA-1 targeting *Circ-XPR1*) and siRNA-2 group (cells transfected with siRNA-2 targeting *Circ-XPR1*). The CCK-8 assay (Solarbio Biotechnology, Beijing, China) was performed to measure cell viability at different time points (1, 2, 3, 4 and 5 days). In brief, an equal number of cells per group was seeded into 96-well plates. The CCK-8 solution (10 μL per well) was then added and incubated at 37 °C for 1 h, and absorbance was measured at 450 nm using a spectrophotometer (Olympus, Tokyo, Japan). The CCK-8 assay was performed in triplicate, and each experiment was repeated three times.

### Luciferase reporter assay

MG-63 or U2OS cells were transfected with a mixture containing 50 ng of firefly luciferase reporter, 5 ng of pRL-CMV Renilla luciferase reporter, and 5 pmol miR-214-5p mimic in a 96-well plate and incubated for 48 h. Luciferase activity was measured using the Dual-luciferase Reporter Assay System (Promega, Madison, Wisconsin, USA). Luciferase activity was normalized against the activity of Renilla luciferase.

### Statistical analysis

All analyses were conducted using SPSS 15.0 statistical software (IBM, SPSS, USA). Data were analyzed by unpaired Students *t* tests for two groups and ANOVA for more than two groups. Correlation analysis between miR-214-5p and Circ-XPR1/*DDX5* was performed using Pearson's correlation analysis. Overall survival (OS) and disease-free survival (DFS) were calculated using Kaplan–Meier survival analysis. *p* values less than 0.05 were considered statistically significant.

## Results

### Identification of Circ-XPR1 by GEO datasets

We first identified differentially expressed circular RNAs according to an online dataset (GSE96964) containing one

human osteoblast hFOB1.19 cell line and seven human osteosarcoma cell lines. Based on fold change ≥ 1 and $p < 0.05$, eight circular RNAs were upregulated, whereas 103 circular RNAs were downregulated (Fig. 1a, b). We validated this data by quantitative reverse transcription-PCR (qRT-PCR) and found that the hsa_circ_0005909 (circ-XPR1) expression level was significantly increased by approximately 3.0-fold in OS tissue compared to control tissue ($p < 0.05$, Fig. 1c).

Circ-XPR1 showed a strong resistance to digestion by RNase R, whereas the linear RNA of *XPR1* was highly degraded (Fig. 1d), indicating that circ-XPR1 is a circRNA. We then used actinomycin D to inhibit transcription of cellular RNA. The abundance of circ-XPR1 was relatively stable until 24 h after treatment with actinomycin D, while *XPR1* was decreased by twofold after 4 h and nearly disappeared within 24 h (Fig. 1e). RNA FISH indicated that circ-XPR1 localized in the cytoplasm, suggesting that circ-XPR1 may regulate gene expression by functioning as a miRNA sponge (Fig. 1f). Total RNA was isolated from nuclear (N) and cytoplasmic (C) fractions, and both circ-XPR1 and XPR1 were preferentially localized within the cytoplasm. Taken together, these results confirmed that circ-XPR1 a stable cytoplasmic circRNA derived from the *XPR1* gene.

Overall survival and disease-free survival were affected by abnormal expression of circ-XPR1 in OS. In OS patients, circ-XPR1 was upregulated and negatively correlated with overall survival and disease-free survival ($p = 0.004$ and $p = 0.025$, respectively; Fig. 1g). According to the genomic structure, exons 8 and 9 in the XPR1 gene are flanked and form the circ-XPR1 on chromosome 1q25.3 (Fig. 1h). Unlike circ-XPR1 expression, the *XPR1* gene was not significantly changed in GSE12865 (Supplement S1 A), which was further verified by RT-PCR (Supplement S1 B).

## Circ-XPR1 promotes OS cell proliferation

To further explore the biological function of circ-XPR1 in OS cell proliferation, we designed two circ-XPR1 oligonucleotides to target the back-splice junction sites (Fig. 2a). MG-63 and U2OS cells transfected with circ-XPR1 siRNA-1 and siRNA-2 showed a significant decrease in cell viability compared to those transfected with control siRNA as assessed by the Cell Counting Kit-8 (CCK-8) assay 4 and 5 days after transfection (Fig. 2b).

Circ-XPR1 siRNA-1 and siRNA-2 inhibited the relative abundance of circ-XPR1 by onefold, while the expression of the *XPR1* linear species was not affected (Fig. 2c). Colony formation assay was used to assess cell proliferation ability, and proliferation was indicated by the number of colonies. The colony formation capacity was reduced in MG-63 and U2OS cells after silencing *circ-XPR1* expression (siRNA-1 and siRNA-2; $p < 0.05$; Fig. 2d).

For circ-XPR1 expression analysis, a circ-XPR1 overexpression vector was constructed and transfected into MG-63 cells via Lipofectamine 2000. Circ-XPR1 was confirmed by abundance analysis (Fig. 2e). CCK-8 analysis demonstrated that MG-63 and U2OS cells overexpressing circ-XPR1 showed increased viability (Fig. 2f). Colony formation assays were consistent with the CCK-8 assays (Fig. 2g). Taken together, these data suggested that circ-XPR1 is a novel circRNA that promotes the proliferation of OS cell lines.

## Circ-XPR1 acts as a sponge of miR-214-5p

To identify a novel potential target for *Circ-XPR1*, we first analyzed the GSE65071 dataset, which includes 20 OS samples and 15 healthy controls. The total number of differentially expressed miRNAs was 164 (78 upregulated miRNAs and 86 downregulated miRNAs; Fig. 3a, b).

By overlapping miRNAs targeting *Circ-XPR1* in the Targetscan and miRanda databases with miRNAs differentially expressed in the GSE65071 dataset, two overlapping miRNAs, miR-214-5p and miR-665, were identified (Fig. 3c). After knockdown Circ-XPR1 expression by two siRNAs, miR-214-5p and miR-665 expression levels were measured. miR-214-5p expression was markedly increased after transfection of siRNA-1 and siRNA-2 (7.85-fold), but miR-665 expression was not significantly increased (1.22-fold increase, Fig. 3d). Circ-XPR1/miR-214-5p interactions were then predicted using circMir (version 1.0), and the targeting site between Circ-XPR1 and miR-214-5p is shown in Fig. 3e.

In total, we identified 17 putative miR-214-5p-binding sites in Circ-XPR1 (Fig. 3f). MiR-214-5p significantly decreased luciferase activity of WT *XPR1* 3′UTR but not Mut *XPR1* 3′UTR (mutant) in MG-63 and U2OS cells (Fig. 3g). Overexpression of circ-XPR1 in MG-63 cells decreased miR-214-5p expression compared to the control group ($p < 0.05$, Fig. 3h).

The relative expression of miR-214-5p was decreased in OS tissues ($n = 20$) compared to control tissues ($n = 20$, Fig. 3i). Spearman's correlation analyses revealed significant negative correlations between circ-*XPR1* and miR-214-5p in OS tissues ($R^2 = 0.435$, $p = 0.002$, Fig. 3j). These findings indicated that circ-XPR1 may act as a sponge to adsorb miR-214-5p.

## miR-214-5p Targets DDX5 in OS Cells

To identify target genes regulated by miR-214-5p, we performed a differentially expressed gene analysis using the GSE12865 dataset, which contains 14 samples (12 osteosarcoma tumor samples and 2 normal human osteoblasts as controls). The array data was background adjusted and

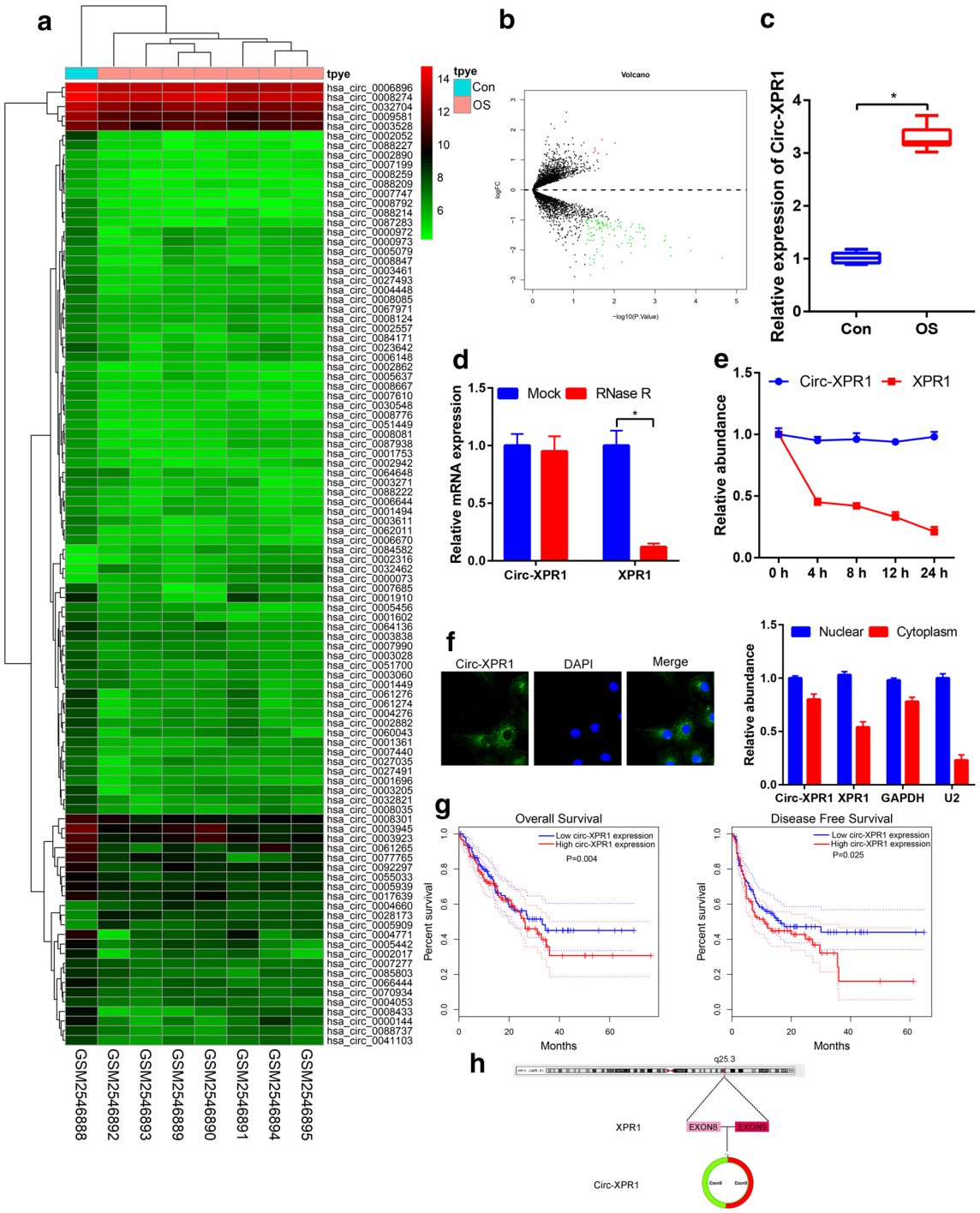


**Fig. 1** Identification of the Circ-XPR1 circular RNA using the GSE96964 dataset. **a** Heatmap of differentially expressed circRNAs between one human osteoblast hFOB1.19 and seven human osteosarcoma cell lines. Green and red represent downregulation and upregulation, respectively. **b** Volcano plots for differentially expressed circRNAs. The red, green and black dots represent downregulation, upregulation and no significance, respectively. **c** Relative expression of Circ-XPR1 in control and OS tissues. **d** Abundance of Circ-XPR1 and linear *XPR1* mRNA treated with RNase R or MOCK as assessed by RT-PCR. **e** Half-life of Circ-XPR1 and *XPR1* after treatment with actinomycin D for 0, 4, 8, 12 and 24 h in MG-63 cells. **f** FISH assay and sublocalization analyses were performed to determine the cellular location of Circ-XPR1. **g** Kaplan–Meier curves of overall survival (OS) and disease-free survival (DFS) of 20 OS patients with low or high Circ-XPR1 expression. **h** Schematic diagram demonstrating that exons 8 and 9 of *XPR1* constitute Circ-XPR1. $*p < 0.05$, Values represent mean ± SD, $n = 3$ independent experiments

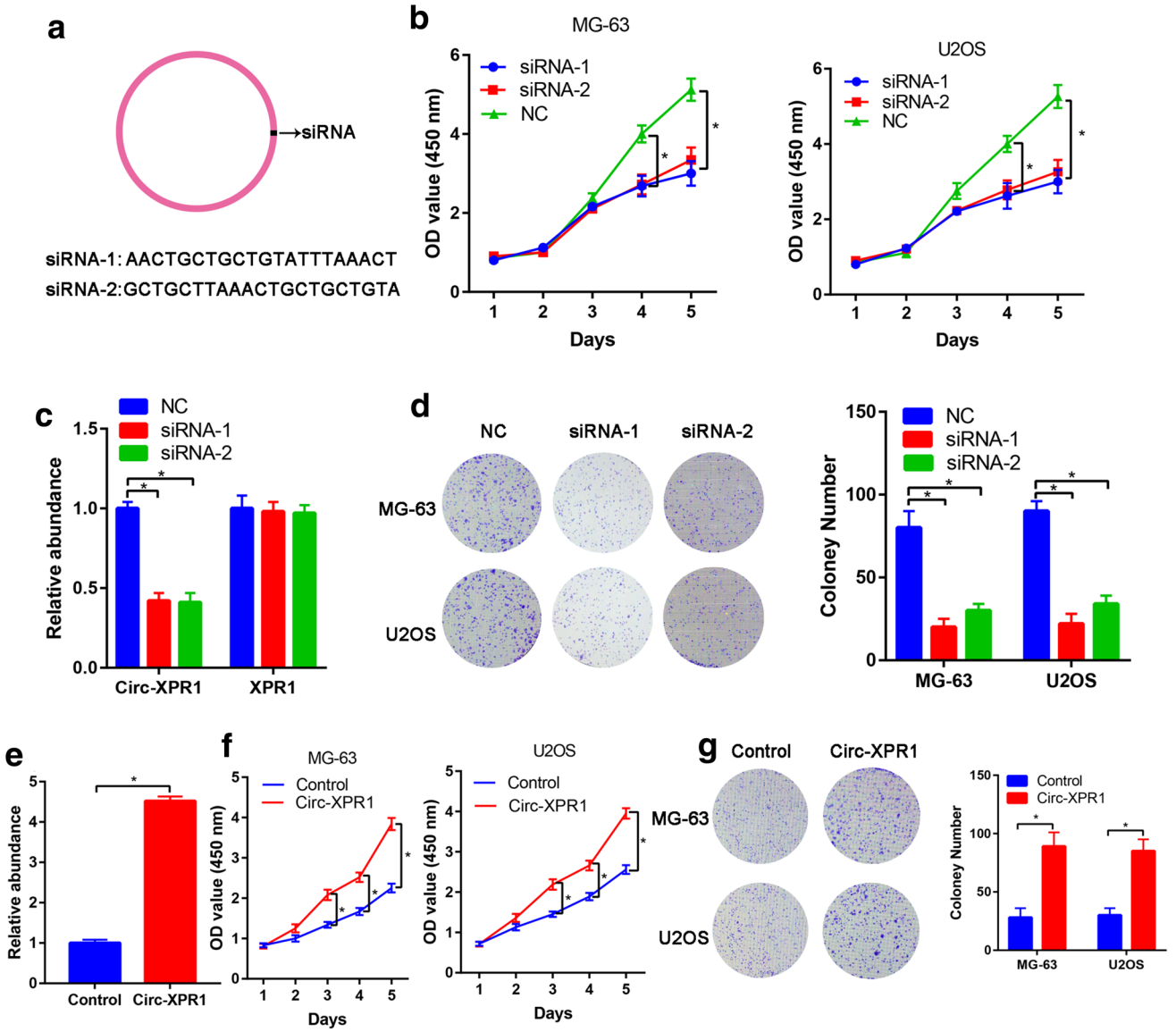


**Fig. 2** Circ-XPR1 promotes the proliferation of OS cells. **a** Schematic representation of the sequence around the back-splice junction site of Circ-XPR1 and the siRNAs targeting the junction site (siRNA-1 and siRNA-2). **b** CCK-8 assays were performed to examine the cell proliferation rate of MG63 and U2OS cells after knockdown of Circ-XPR1 by siRNA-1 and siRNA-2 at 1, 2, 3, 4 and 5 days. **c** Relative abundance of Circ-XPR1 and XPR1 expression in MG-63 cells after transfection with Circ-XPR1 siRNA-1 and siRNA-2. **d** Colony formation assays showed decreased colony formation ability after Circ-XPR1 knockdown in MG-63 and U2OS cells. **e** Relative abundance of Circ-XPR1 in MG-63 cells after transfection with Circ-XPR1 plasmids. **f** Cell proliferation was measured by CCK-8 at 1, 2, 3, 4 and 5 days after transfection of Circ-XPR1 and control plasmids. **g** Colony formation assays showed decreased colony formation ability after overexpression of Circ-XPR1 in MG-63 and U2OS cells. $*p < 0.05$, Values represent mean ± SD, $n = 3$ independent experiments

normalized using the mean-centering approach in R software (Fig. 4a). We generated a volcano plot (Fig. 4b) and heat map (Fig. 4c) showing differential gene expression between control and OS samples. We overlapped three miRNA target gene databases (Targetscan, https://www.targetscan.org/mamm_31/; miRBase, https://www.mirbase.org/ and RNAhybrid, https://bibiserv.techfak.uni-bielefeld.de/rnahybrid/) and one dataset from the GEO database (GSE12865). Four genes, namely, *DDX5, CPA4, NRG1,* and *CCBE1*, were identified as shown in Fig. 4d.

The free energy value of miR-214-5p to its target binding site ranged from -15.34 to − 38.9 kcal/mol, and the binding free energy for *DDX5* was maximum. Thus, *DDX5* was selected for further investigation. Putative target genes of miR-214-5p were predicted by bioinformatics analysis using miRNA target prediction software (Targetscan, https

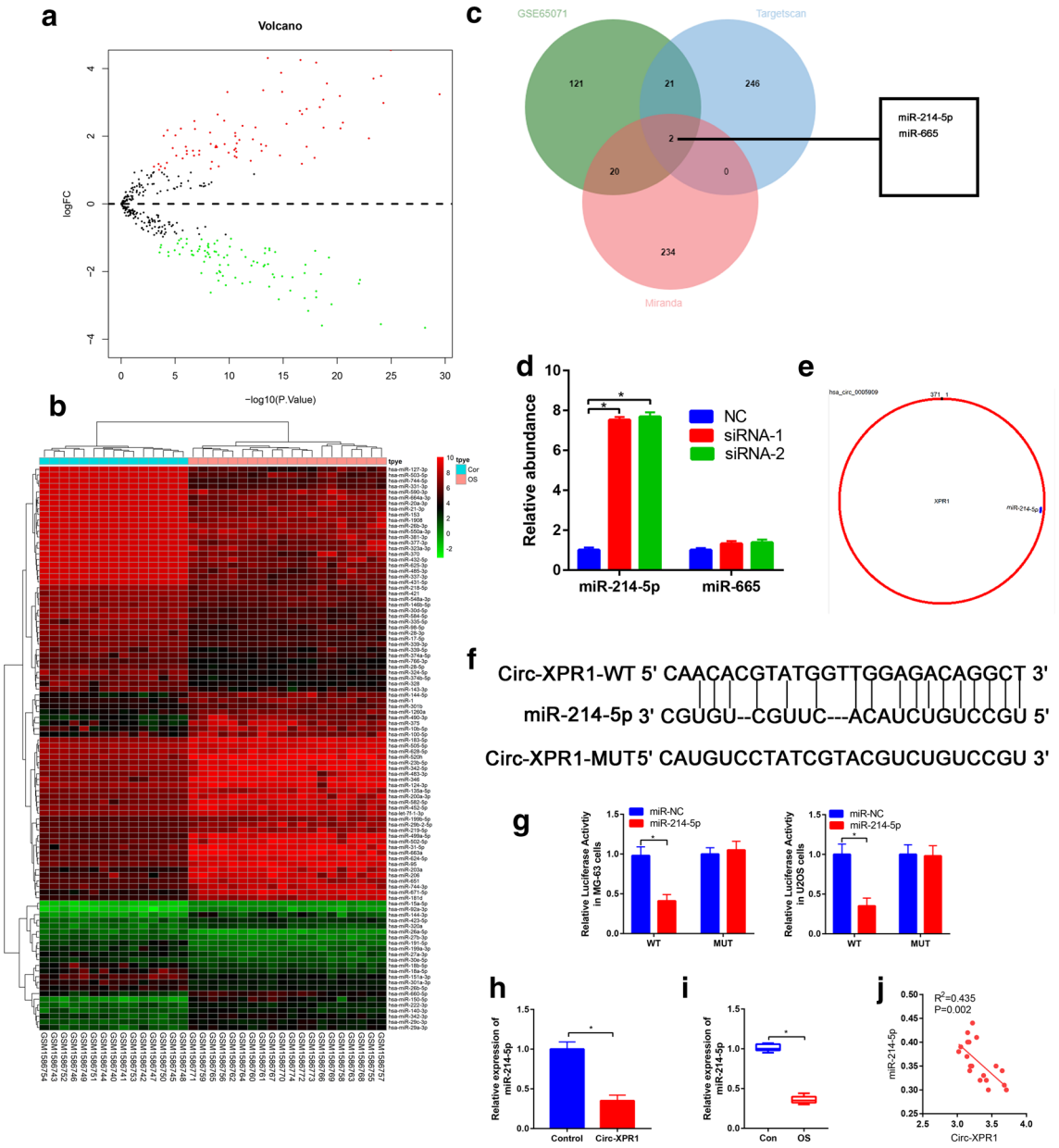


**Fig. 3** Circ-XPR1 acts as a miR-214-5p sponge in OS cells. **a** GSE65071 was used to evaluate differentially expressed miRNAs between OS and control samples. The significant genes are shown by a volcano plot with a threshold of fold change ≥ 1 and $p$ value < 0.05. The red, green and black dots represent the downregulation, upregulation, and no significance, respectively. **b** Heatmap of the differentially expressed miRNAs between OS and control samples. Green and red represent downregulation and upregulation, respectively. **c** Two miRNAs (miR-214-5p and miR-665) were identified by Venn analysis of GSE65071, Targetscan and miRanda databases. **d** Relative abundance of miR-214-5p and miR-665 in MG-63 cells after transfection with siRNA-1 or siRNA-2 and NC. **e** Schematic illustration of the Circ-XPR1- and miR-214-5p-binding sites. **f** The potential miR-214-5p-binding site of Circ-XPR1-WT. **g** Relative luciferase activity was analyzed for WT or Mut 3′-UTR *XPR1* reporter plasmids cotransfected with miR-214-5p mimic or miR-NC. **h** Relative expression of miR-214-5p after transfection of Circ-XPR1 plasmids and control plasmid. **i** Relative expression of miR-214-5p in OS and control tissues. **j** Correlation between Circ-XPR1 and miR-214-5p in OS tissues ($R^2 = 0.435$, $p = 0.002$). *$p < 0.05$, Values represent mean ± SD, $n = 3$ independent experiments

://www.targetscan.org/mamm_31/). Furthermore, a dual-luciferase reporter assay revealed that *DDX5* is a putative target of miR-214-5p (Fig. 4e).

The dual-luciferase reporter assay revealed that miR-214-5p decreased the luciferase activity of WT-*DDX5* but did not affect the luciferase activity of MUT-*DDX5* in

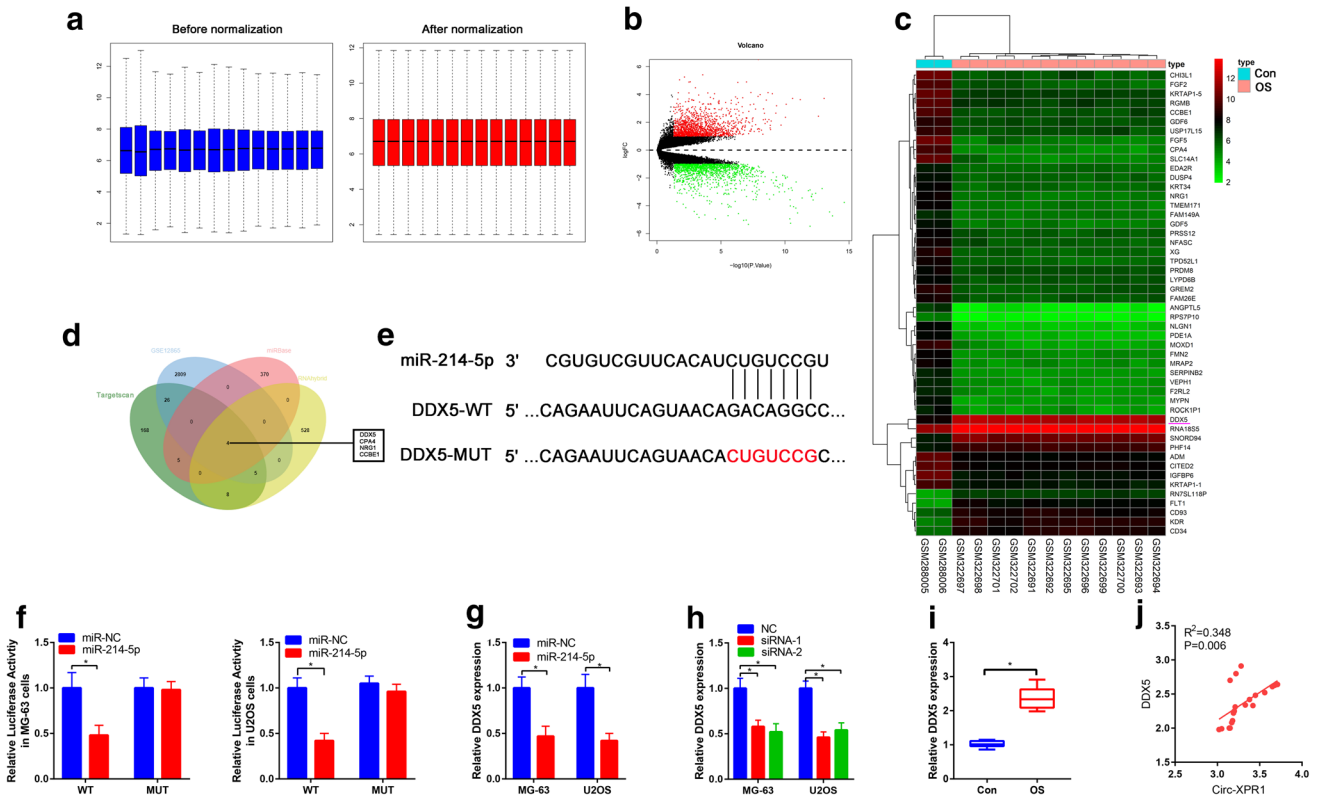


**Fig. 4** *DDX5* is a target of miR-214-5p in OS cells. **a** Comparison of the expression value before normalization and after normalization of GSE12865. **b** Volcano plot of differentially expressed genes in GSE12865. The red, green and black dots represent downregulation, upregulation, and no significance, respectively. **c** Heat map displaying differential mRNA expression in OS within the GSE12865 dataset. Color scale at right side of heatmap shows the expression level. Red indicates upregulation, and green indicates downregulation. **d** Venn diagram demonstrates the intersection genes from GEO dataset (GSE12865), Targetscan, miRbase, and RNAhybrid. **e** Prediction of the binding sites between miR-214-5p and *DDX5*. **f** Relative luciferase activity following cotransfection of miR-214-5p mimic with *DDX5* 3′UTR WT or MUT in MG-63 and U2OS cells. **g** Relative expression of DDX5 in miR-214-5p mimic and miR-NC groups in MG-63 and U2OS cells. **h** Relative expression of *DDX5* in MG-63 and U2OS cells after transfection with Circ-XPR1 siRNA-1 and siRNA-2. **i** Relative expression of *DDX5* in OS and control tissues. **j** Correlation analysis between Circ-XPR1 and *DDX5* ($R^2 = 0.348$, $p = 0.006$). $^*p < 0.05$, values represent mean ± SD, $n = 3$ independent experiments

MG-63 and U2OS cells (Fig. 4f). Furthermore, we measured the expression of DDX5 in the miR-214-5p and negative control groups. As shown in Fig. 4g, the expression of DDX5 rapidly decreased in response to miR-214-5p, but miR-214-5p NC expression did not decrease significantly in MG-63 and U2OS cells. After transfection of two siRNAs targeting circXPR1, *DDX5* expression was significantly decreased in MG-63 and U2OS cells (Fig. 4h). The expression level of *DDX5* was significantly upregulated in OS tissues compared to control tissues ($p < 0.05$, Fig. 4i). Furthermore, circXPR1 and *DDX5* were also positively correlated ($R^2 = 0.348$, $p = 0.006$, Fig. 4j). Western blot assay revealed that miR-214-5p decreased *DDX5* protein expression in MG-63 and U2OS cells (Fig. 5a). Knockdown of circXPR1 also decreased DDX5 protein expression in MG-63 and U2OS cells (Fig. 5b). Furthermore, *DDX5* protein expression was upregulated in OS tissues compared to control tissues (Fig. 5c). These findings indicated that the *DDX5* gene is the target of miR-214-5p.

## Discussion

In this study, we first identified circ-XPR1 as a key upregulated circRNA involved in OS cell proliferation. In addition, gain- and loss-of-function experiments confirmed that circ-XPR1 promotes OS cell proliferation. For the first time, we identified and verified the role and potential function of circ-XPR1 in OS progression. Circ-XPR1 is derived from exons 8 and 9 within the *XPR1* gene locus. *XPR1* is a 696-amino acid protein and has been identified to play a vital role in tumor progression [14]. In this study, we used a GEO dataset to investigate differentially expressed circRNAs in OS and identified a novel circRNA, namely, Circ-XPR1.

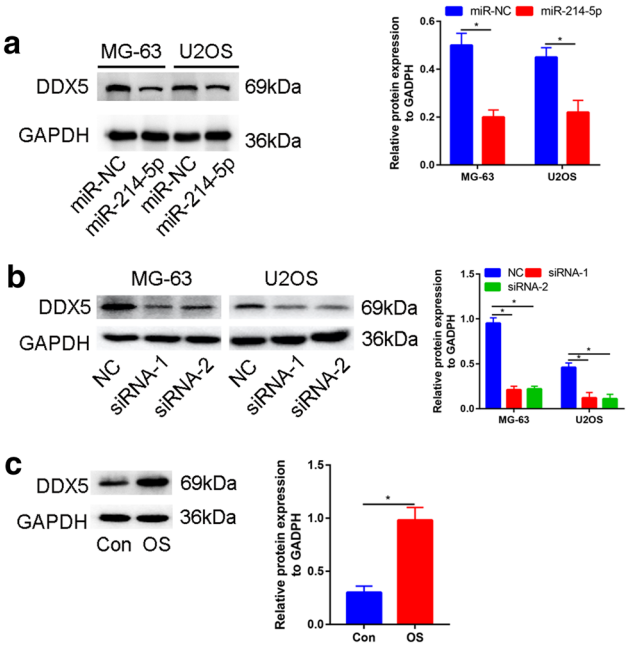


**Fig. 5** *DDX5* protein expression in OS tissues and cells. **a** Western blot assay assessed *DDX5* protein expression in miR-214-5p-transfected OS cells. **b** *DDX5* protein expression in OS cells transfected with circ-XPR1 siRNA. **c** *DDX5* protein expression in OS and control tissues. $^{*}p < 0.05$, values represent mean ± SD, $n = 3$ independent experiments

Circ-XPR1 was upregulated in OS tissue and associated with shorter overall survival rates. Subcellular fractionation assay and RNA FISH showed that Circ-XPR1 mainly accumulated in the cytoplasm, suggesting that Circ-XPR1 might act as a sponge of miRNAs to regulate gene expression and OS progression.

We used a GEO dataset to identify, differentially expressed miRNAs, and two putative target miRNAs of Circ-XPR1 were selected by the intersection of two databases and the GEO dataset. Circ-XPR1 contains a conserved miR-214-5p target site that was validated by a dual-luciferase reporter gene assay, miRNA abundance analysis and correlation analyses. miR-214-5p has multiple biological functions, including inhibition of proliferation in nonsmall lung cancer [15], cervical cancer [16] and esophageal cancer [17]. The results of this study were similar to those of previous studies demonstrating that miR-214-5p is downregulated in OS tissues and may possess antitumor effects [18, 19]. Zhang et al. [18] demonstrated that miR-214-5p targets ROCK1 and suppresses proliferation and invasion of human OS cells. Moreover, Zhou et al. [19] performed in vivo and in vitro studies, which demonstrated that LINC00612 functions as a ceRNA for miR-214-5p to promote OS cell invasion.

To identify the targets of miR-214-5p, we preprocessed the gene expression profiles collected from the GEO database (GSE12865), resulting in 2839 genes. Four putative target mRNAs of miR-214-5p were selected by the intersection of three databases and GSE12865. A luciferase reporter assay revealed that miR-214-5p inhibited DDX5-WT activity, suggesting that DDX5 is directly targeted by miR-214-5p.

*DDX5*, a nuclear prototypic member of the DEAD box family, is abnormally expressed in a variety of malignancies, including neuroblastoma [20], breast cancer [21], prostate cancer [22] and colorectal cancer [23]. In addition, silencing of *DDX5* by siRNA blocks the migration of carcinoma cells [24]. Chen et al. [25] reported that lncRNA DLEU1 sponges miR-671-5p and upregulates DDX5 expression to aggravate OS carcinogenesis, suggesting that *DDX5* promotes the occurrence and development of OS.

The expression level of *DDX5* in OS tissue samples was significantly increased and positively correlated with Circ-XPR1 expression. Therefore, we propose that the Circ-XPR1/miR-214-5p/*DDX5* axis is a novel target for OS progression. However, these results do not preclude the possibility that other potential target genes are involved in OS progression. Future investigations should aim to further reveal the regulatory role of the CircXPR1/miR-214-5p/*DDX5* axis in OS in vivo.

## Conclusion

In summary, we identified a novel circRNA derived from the *XPR1* gene. We demonstrated that Circ-XPR1 acts as tumor promotion factor through regulating the miR-214-5p/*DDX5* axis in OS. Our study demonstrated that Circ-XPR1 may be a potential target for therapeutic intervention of OS.

**Author contributions** XM and SG performed the majority of experiments and analyzed the data; LG and GL performed the molecular investigations; LH and GL designed and coordinated the research; XM and SG wrote the full texts.

**Funding** This research did not receive any specific grant from funding agencies in the public, commercial, or not-for-profit sectors.

## Compliance with ethical standards

**Conflict of interest** The authors declared that they have no conflicts of interest to this work.

**Ethical approval and consent to participate** The specimens of osteosarcoma and adjacent tissues were collected from the patients who were diagnosed with osteosarcoma in Henan Provincial People's Hospital. The informed consents for each patient were obtained and the procedures were approved by the Ethics Committee of Henan Provincial People's Hospital (Approval no. 2020071203).

## References


1. Zhang HP, Yu ZL, Wu BB, Sun FR. PENK inhibits osteosarcoma cell migration by activating the PI3K/Akt signaling pathway. J Orthop Surg Res. 2020;15:162.
2. Mirabello L, Troisi RJ, Savage SA. Osteosarcoma incidence and survival rates from 1973 to 2004: data from the surveillance, epidemiology, and end results program. Cancer. 2009;115:1531–43.
3. Gu Z, Wu S, Wang J, Zhao S. Long non-coding RNA LINC01419 mediates miR-519a-3p/PDRG1 axis to promote cell progression in osteosarcoma. Cancer Cell Int. 2020;20:147.
4. Ding WZ, Liu K, Li Z, Chen SR. A meta-analysis of prognostic factors of osteosarcoma. Eur Rev Med Pharmacol Sci. 2020;24:4103–12.
5. Du Q, Zhang W, Feng Q, Hao B, Cheng C, Cheng Y, Li Y, Fan X, Chen Z. Comprehensive circular RNA profiling reveals that hsa_circ_0001368 is involved in gowth hormone-secreting pituitary adenoma development. Brain Res Bull. 2020;161:65–77.
6. Wang HY, Wang YP, Zeng X, Zheng Y, Guo QH, Ji R, Zhou YN. Circular RNA is a popular molecule in tumors of the digestive system (Review). Int J Oncol. 2020;57:21–422.
7. Fang Y, Long F. Circular RNA circ_0000337 contributes to osteosarcoma via the iR-4458/BACH1 pathway. Cancer Biomark. 2020;28:411–9.
8. Zhang PR, Ren J, Wan JS, Sun R. Circular RNA hsa_circ_0002052 promotes osteosarcoma via modulating miR-382/STX6 axis. Hum Cell. 2020;33:810–8.
9. Zhu ST, Wang X, Wang JY, Xi GH, Liu Y. Downregulation of miR-22 contributes to epithelial-mesenchymal transition in osteosarcoma by targeting Twist1. Front Oncol. 2020;10:406.
10. Liu WG, Zhuo L, Lu Y, Wang L, Ji YX, Guo Q. MiR-874–3p inhibits cell migration through targeting RGS4 in osteosarcoma. J Gene Med. 2020;10:e3213.
11. Gautier L, Cope L, Bolstad BM, Irizarry RA. affy–analysis of Affymetrix GeneChip data at the probe level. Bioinformatics. 2004;20:307–15.
12. Irizarry RA, Hobbs B, Collin F, Beazer-Barclay YD, Antonellis KJ, Scherf U, Speed TP. Exploration, normalization, and summaries of high density oligonucleotide array probe level data. Biostatistics. 2003;4:249–64.
13. Smyth GK. Linear models and empirical bayes methods for assessing differential expression in microarray experiments. Stat Appl Genet Mol Biol. 2004;3:1–25.
14. Chen WC, Li QL, Pan Q, Zhang HY, Fu XY, Yao F, Wang JN, Yang AK. Xenotropic and polytropic retrovirus receptor 1 (XPR1) promotes progression of tongue squamous cell carcinoma (TSCC) via activation of NF-κB signaling. J Exp Clin Cancer Res. 2019;38:167.
15. Chen YR, Wu YS, Wang WS, Zhang JS, Wu QG. Upregulation of lncRNA DANCR functions as an oncogenic role in non-small lung cancer by regulating miR-214-5p/CIZ1 axis. Eur Rev Med Pharmacol Sci. 2020;24:2539–47.
16. Guo M, Lin B, Li G, Lin J, Jiang X. LncRNA TDRG1 promotes the proliferation, migration, and invasion of cervical cancer cells by sponging miR-214-5p to target SOX4. J Recept Signal Transduct Res. 2020;40:281–93.
17. Liu HF, Zhen Q, Fan YK. LINC00963 predicts poor prognosis and promotes esophageal cancer cells invasion via targeting miR-214-5p/RAB14 axis. Eur Rev Med Pharmacol Sci. 2020;24:164–73.
18. Zhang M, Wang D, Zhu T, Yin R. miR-214-5p targets ROCK1 and suppresses proliferation and invasion of human osteosarcoma cells. Oncol Res. 2017;25:75–81.
19. Zhou Y, Li X, Yang H. LINC00612 functions as a ceRNA for miR-214-5p to promote the proliferation and invasion of osteosarcoma in vitro and in vivo. Exp Cell Res. 2020;392:112012.
20. Zhao X, Li D, Yang F, Lian H, Wang J, Wang X, Fang E, Song H, Hu A, Guo Y, Liu Y, Li H, Chen Y, Huang K, Zheng L, Tong Q. Long noncoding RNA NHEG1 Drives β-Catenin transactivation and neuroblastoma progression through interacting with DDX5. Mol Ther. 2020;28:946–62.
21. Hashemi V, Masjedi A. The role of DEAD-box RNA helicase p68 (DDX5) in the development and treatment of breast cancer. J Cell Physiol. 2019;234:5478–87.
22. You Z, Liu C, Wang C, Ling Z, Wang Y, Wang Y, Zhang M, Chen S, Xu B, Guan H. LncRNA CCAT1 promotes prostate cancer cell proliferation by interacting with DDX5 and MIR-28-5P. RNA Biol. 2019;18:2469–79.
23. Dai L, Pan G, Liu X, Huang J, Jiang Z, Zhu X, Gan X, Xu Q, Tan N. High expression of ALDOA and DDX5 are associated with poor prognosis in human colorectal cancer. Cancer Manag Res. 2018;10:1799–806.
24. Quan Z, Zhang BB, Yin F, Du J, Zhi YT, Xu J, Song N. DDX5 silencing suppresses the migration of basal cell carcinoma cells by downregulating JAK2/STAT3 pathway. Technol Cancer Res Treat. 2019;18:1533033819892258.
25. Chen X, Zhang C, Wang X. Long noncoding RNA DLEU1 aggravates osteosarcoma carcinogenesis via regulating the miR-671-5p/DDX5 axis. Artif Cells Nanomed Biotechnol. 2019;47:3322–8.